

Virtual material approach to self-healing CMCs

Guillaume Couégnat*, Gerard L. Vignoles *, Virginie Dréan**, Christianne Mulat****, William Ros****, Grégory Perrot***, Thomas Haurat*, Jalal El-Yagoubi*, Eric Martin*, Mario Ricchiuto**, Christian Germain*** and Michel Cataldi****

* University Bordeaux, Lab. for ThermoStructural Composites (LCTS)

3, Allée La Boétie, F33600 PESSAC, France

** University Bordeaux, INRIA Sud-Ouest

350 Cours de la Libération, F33410 Talence Cedex, France

*** University Bordeaux, Inst. of Integration from Materials to Systems (IMS)

350 Cours de la Libération, F33410 Talence Cedex, France

****Safran-Snecma Propulsion Solide

Les Cinq Chemins, 33185 Le Haillan, France

Abstract

We introduce an integrated software suite aiming at a numerical simulation of the whole life of Self-healing Ceramic-Matrix Composites (CMCs) materials, featuring: (i) reinforcement weaving, (ii) matrix infiltration, (iii) mechanical behaviour including damage, (iv) thermal behaviour, and (v) self-healing under oxidative gases. All simulations are developed in strong relationship with image analysis and synthesis. Preliminary results are presented and discussed.

1. Introduction

Self-healing Ceramic-Matrix Composites (CMCs) are promising candidates for, among other applications, civil jet engine hot parts [1]. Their behaviour in actual conditions of use has been characterized experimentally, showing excellent lifetimes [2]. They are constituted of a woven/interlocked 3D arrangement of SiC fibre tows, infiltrated by a multilayer matrix. All the interphase and matrix layers have a specific role: (i) a pyrocarbon interphase acts as a crack deviator and prevents premature fibre failure while the matrix undergoes multiple cracking, *i.e.* progressive damage; (ii) SiC matrix layers bring stiffness and are chemically inert at moderate temperatures, (iii) boron-containing phases are able to produce above 450°C a liquid oxide which fills cracks and prevents further oxidation by a diffusion barrier effect. [3]

The large-scale industrial fabrication of such materials will be economically possible if the fabrication expenses are cut down, while guaranteeing sufficient life duration. In this aim, optimization of the material by varying its organization parameters, *i.e.* weaving patterns, layered matrix design (number, thicknesses, etc...) is a key issue. Unfortunately, the production of samples is very lengthy and expensive. This is why a modelling approach looks attractive: a prediction of the variation of the material properties when changing some design parameter would be fast and inexpensive provided it is reliable enough.

The most important points for reliability are the accuracy in the description of the materials architecture on the one hand, and of the physical, mechanical and chemical phenomena on the other hand. To address this, all simulations presented here are in strong relationship with image analysis and synthesis, in order to provide a sound basis for experimental validation with respect to actual material samples. The materials structure is observed and the resulting information is utilized either directly or indirectly for simulations of the materials life. A class of realistic methods is to perform direct simulations inside accurate 3D representations of the material, such as those produced by ultrasound or tomographic investigations [4]; however, the question of the representativity of the scanned sample is not addressed in this way, unless the procedure is repeated many times on many samples. On the other hand, it is always possible to start from “ideal” representations of the material, *e.g.* descriptions by a collection of geometrical objects arranged in space, but the doubt resides in how far the model is from the actual material. Undoubtedly, an integrative approach has to bridge these two extremes. Actually, an *a priori* representation should include as many parameters as possible to account for the “non-ideality” of the materials geometry, and these parameters have to be identified from the analysis of a large enough number of sample images. Yet, direct simulations are of interest since they allow capturing effects that could be missed in an *a priori* approach of the material.

In addition to these elements, since the material architecture is organized upon several length scales, multi-scale analysis and change-of-scale methods have to be performed.

2. Methods

The numerical tools have been developed either on structured or on unstructured meshes. Indeed, in some cases, unstructured meshes are of larger interest, for example, in the case of ideal structure design; while on the other hand, if one starts from a real 3D image of the material structure, structured meshes like regular 3D grids are of easier use. Since our computational tools are compatible with regular or irregular meshes, we have developed converters capable of *e.g.* creating a voxel grid from an unstructured FE mesh. In this way, exchange between these two kinds of material representations is made possible.

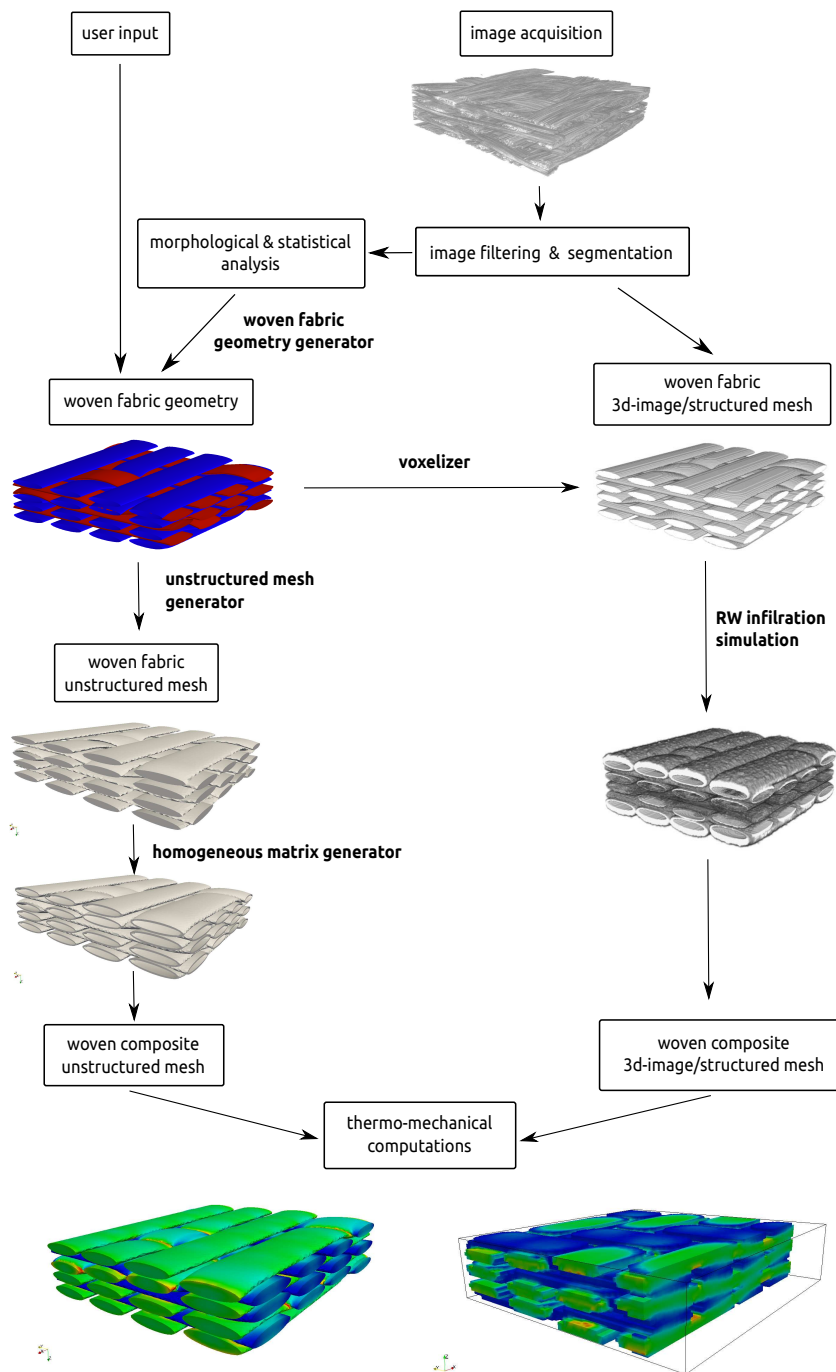


Figure 1. Virtual material approach at large scale (fabric scale).

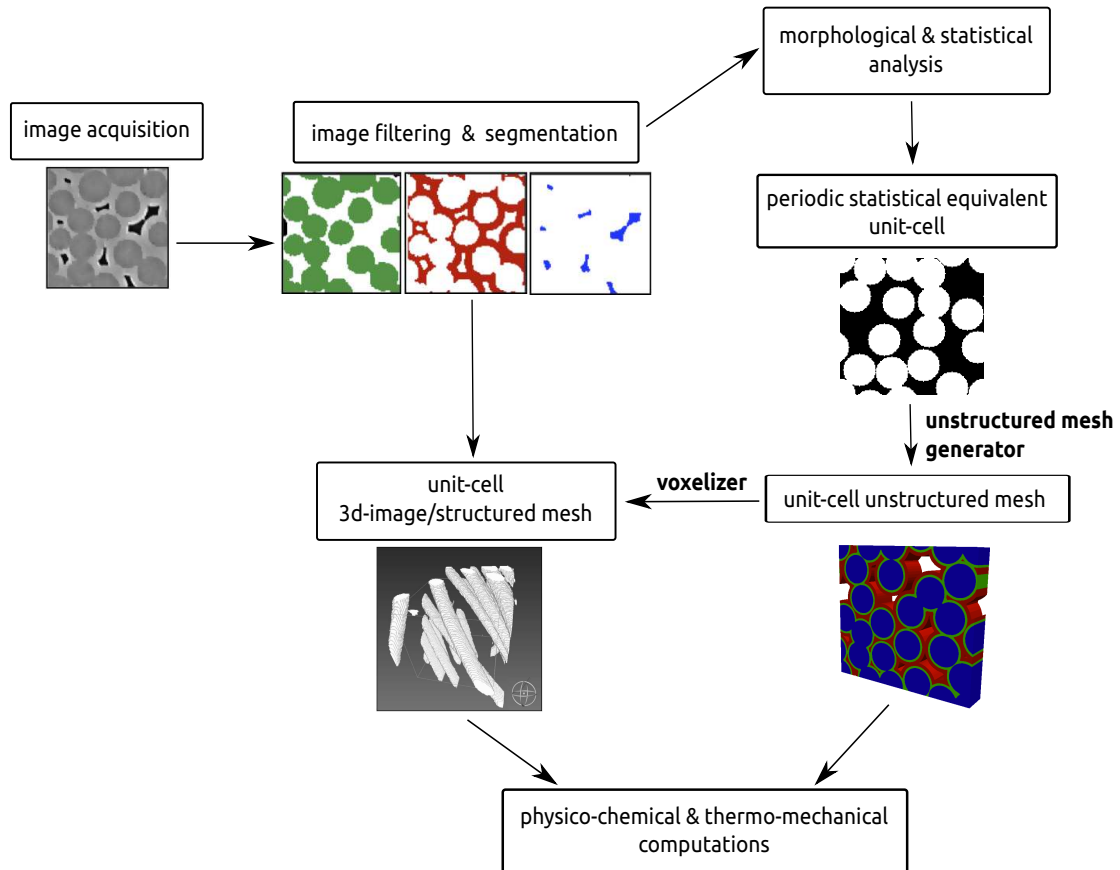


Figure 2. Virtual material approach at small scale (fiber scale)

Figures 1 and 2 respectively show how the approach is structured at large and small scale; large similarities are present, though the material geometries and the details of the physics are distinct. One of the crucial points is the possibility to work either from acquired images, which allows validation of the computations, or with direct user input, which confers the software package the character of a material design toolbox.

2.1 Reinforcement weaving design

The fibrous reinforcement of CMC is usually made of a textile woven fabric of carbon or ceramic fibers. The weaving patterns range from simple 2D fabric (as twill or satin) to more complex 3D multilayered interlock weaves. A dedicated modeling package [5] has been developed allowing automatic generation of solid models for woven reinforcements (Figure 3). The internal geometry of the textile fabric is retrieved from the weaving pattern and basic geometric data about the yarns (cross section shape, thickness, etc.). The yarns interactions are deduced from the topology of the fabric, and the positions of their centerlines are then computed between each crossing points using an energy minimization procedure. The resulting geometric model can then be converted to either an unstructured or a structured mesh. The meshing process is straightforward since the underlying geometric model guarantees that no interpenetration occurs between the yarns entities. Moreover, the local material properties are assigned automatically depending on the local crimp angle of the yarns. In the current geometric approach, the yarns are considered as rigid entities, not accounting for the experimentally observed changes of their cross sections [6-Boisse!]. An on-going development consists in a more realistic representation as an intermediate fibrous model built upon the geometric one. The yarns entities are decomposed as sets of individual “macro-fibres” and the initial fabric geometry is relaxed using a dynamic relaxation algorithm to simulate the tensile load applied to the fabric during the weaving process. Contact and friction forces between each individual “macro-fibres” are evaluated, which leads to yarns compaction, cross-section changes and fibres reorientations, as illustrated in Figure 3.

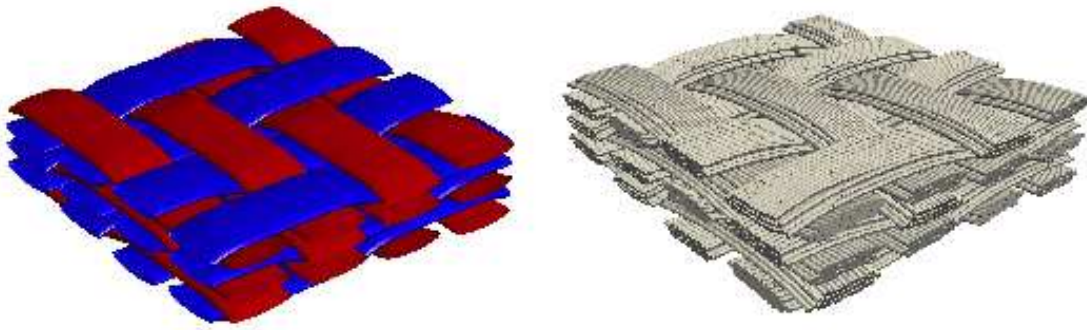


Figure 3. Geometric model (left) and intermediate fibrous representation (right) of a woven multilayered fabric.

2.2 Design of the fibre arrangement in the tows

The arrangement of fibres in the tow, as opposed to the arrangement of the tows in the fabric, does not apparently follow a rigorous geometrical specification – rather, it appears more as a random process. So, in this work, the characteristics of this random arrangement have been extracted from the actual material by image analysis. In the case of carbon fibres, this is rather a difficult task, which has led to specific image processing developments [7-8]. Then, in a 2D perpendicular view of the tow, the fibres are identified, and their quasi-random arrangement is characterized using a two-point probability function as a statistical descriptor. Based on this descriptor, spatial correlation and length scales of the microstructure could be inferred. Statistical equivalent unit cells could then be generated using this information: starting from a random initial configuration, fibres positions are optimized so that the two-point probability function of the unit cell replicates the one of the initial microstructure, and that the fibres are eventually forbidden to overlap. This ensures that the reconstructed unit cells exhibit both the expected volume fraction and microstructure characteristic lengths. An automatic meshing procedure has also been developed to produce unstructured meshes of complete unit cells, *i.e.* including interphase material and one or several layer of matrix around the fibres. [9]

3. Simulations : methods and results

3.1 Matrix infiltration simulation

Two levels of detail for the simulation of matrix infiltration by isothermal Chemical Vapour Infiltration (I-CVI) have been implemented.

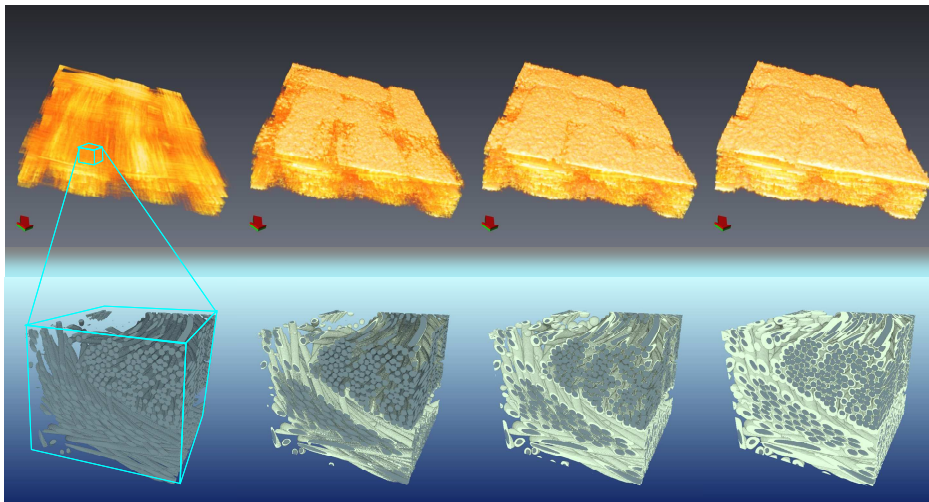


Figure 4. Macro-scale (top) and micro-scale (bottom) infiltration modelling by random walkers. Depending on the physicochemical conditions, there appear matrix thickness gradients at small scale (bottom right). The macro-scale code simultaneously handles intra-tow infiltration and seal-coat deposition (top right).

The first-level model consists in filling the virtual tows by a constant amount of matrix, and in covering them by a seal-coat layer with constant thickness (see figure 1, left). For unstructured mesh representations of the woven fabric, this simulation is performed by Boolean operations directly on meshes.

A second level of simulation involves the actual physico-chemical modelling of chemical vapour infiltration. A two-scale approach has been developed, based on X-ray CMT images or on synthesized 3D images discretized on a regular voxel grid [10]. An intra-tow code allows for the precise simulation of the matrix deposition [11-12]; the deposit thickness variations are shown to depend on (i) the diffusion-reaction competition, which implies a smaller deposit thickness in small pores, and (ii) the pore network connectivity. The results are interpreted as local laws for effective parameters (diffusivity, bulk reactivity) [13] in a large-scale solver based on Brownian motion [14], capable of simultaneously computing the matrix phase amount in the tows and the seal-coat matrix thickness outside the tows. This code takes into account the local values of the volume fraction and of the orientation of the fibres.

Both codes have been validated with respect to experimental data [11,14] in the case of Carbon-carbon composite fabrication; they are currently being applied to SH-CMCs, as illustrated on Figures 1 (right) and 4.

3.2 Elasticity and damage

The generated micro- and meso-scale cell meshes of a CMC material could be used to evaluate its initial and effective thermo-mechanical properties during its lifetime at both scales. Once the meshes are constructed and the local materials properties are assigned to the elements, the effective mechanical properties can be computed in a relatively straightforward manner using elastic finite element calculation. However, the large size of the resulting meshes motivates the use of advanced numerical tools like parallel direct solver to keep the computation time acceptable.

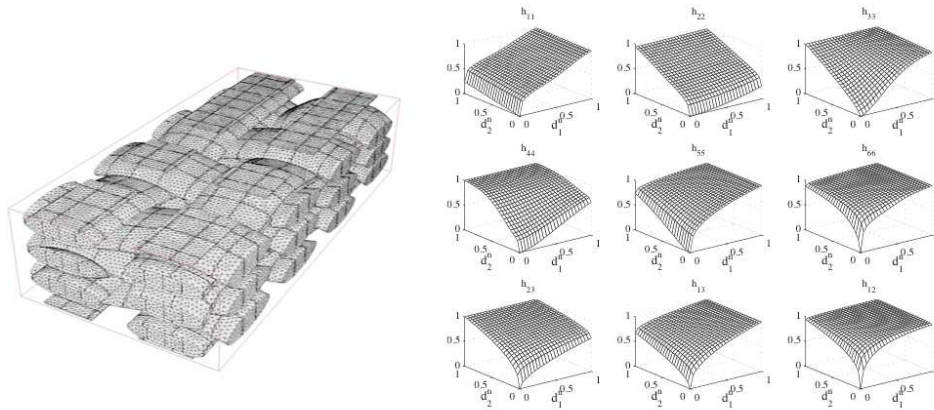


Figure 5. A woven CMC unstructured mesh with cracks used to evaluate the damage effect tensor (left) and the corresponding evolution of the elasticity tensor components as functions of the matrix cracks densities in reinforcement directions (right)

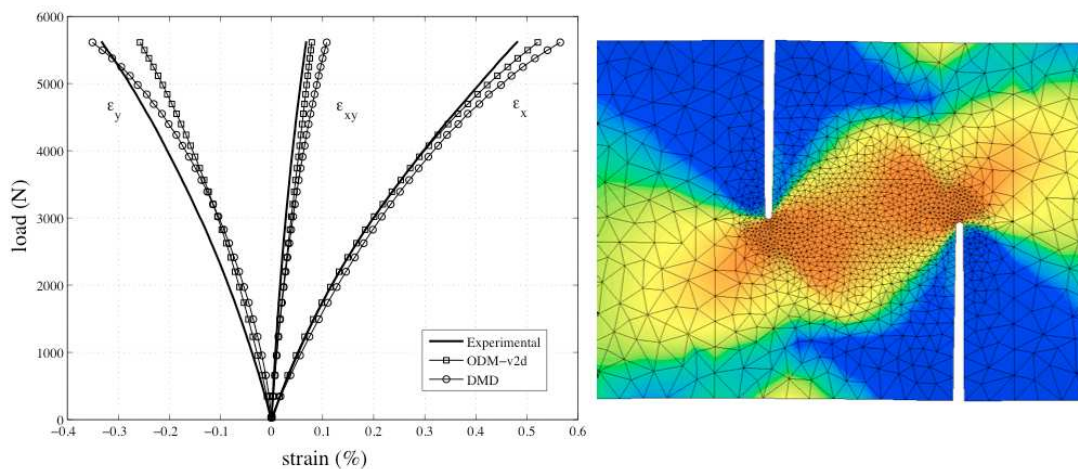


Figure 6. Simulation of a 45° off-axis tensile test on a woven C/SiC shifted-notched specimen: left – comparison between the experimental response and the ones simulated using a purely macroscopic model (square) and the multiscale DMD model (circle), right – simulated matrix crack density map with the DMD model.

As mentioned previously, CMC materials exhibit progressive damage when they are subjected to a thermo-mechanical loading. To evaluate the effect of this damage on the effective mechanical properties, cracks and debonding corresponding to experimentally observed damage states are inserted directly into the FE meshes (Figure 5, left) and the same homogenization procedure is performed on the damage cells. The evolution of the complete elasticity tensor could then be retrieved as response surfaces for any damage state by interpolation (Figure 5, right). The numerical evaluation of the so-called damage effect tensor also served as a basis for the development of a multiscale damage model (DMD) [15,16], where the crack densities and the debonding lengths are directly used as the damage variables. The effective material behavior model is written in a classical macroscopic framework, but it benefits from the multiscale nature of the damage effect tensor and thus allows access to the evolution of the material microstructure at the large (fabric) scale. Figure 6 shows an excellent agreement on a 45° off-axis tensile test on a notched C/SiC sample.

3.3 Thermal behaviour

The main thermal property to be evaluated is the heat conductivity, or alternatively, the heat diffusivity, since the heat capacity may be easily computed and measured. This may be carried out from the knowledge of the individual properties of the components and of their arrangement by several averaging methods. One of them is periodic homogenization [17], which can be straightforwardly implemented in finite elements, requiring only the definition of a periodic representative unit cell. Again, an image-based method has allowed confirming the correlation between the damage state in a CMC (*i.e.* crack density and opening width) and its thermal conductivity [18], as shown in Figure 7, since cracks are thermal barriers.

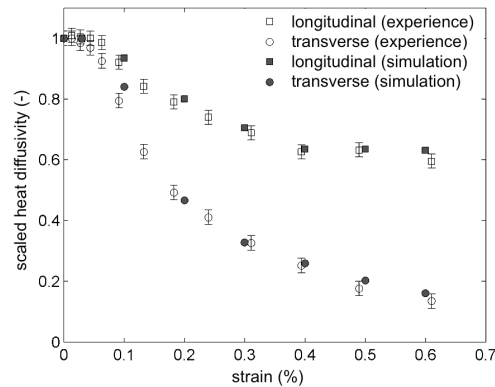


Figure 7. Experimental and simulated evolution of the heat diffusivity of a SiC/SiC woven CMC under tensile loading.

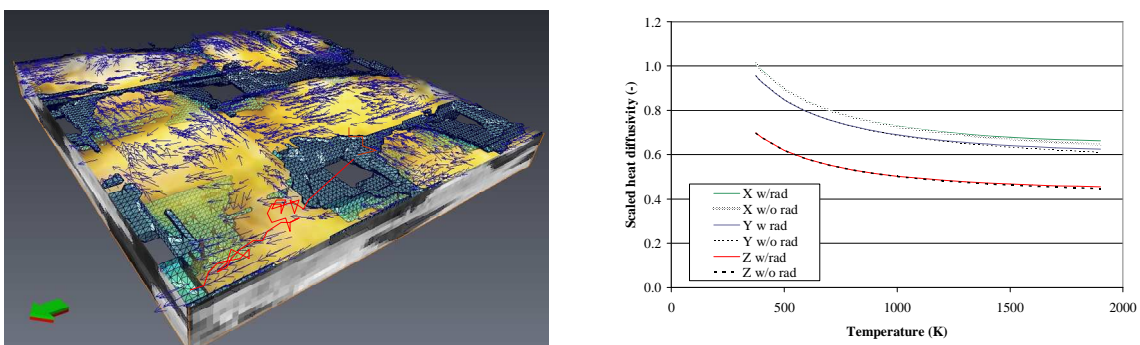


Figure 8. Simulation of coupled radiative and conductive (diffusive) heat transfer by hybrid random walks in a 3D image of a CMC obtained by X-ray CMT. Left: the 3D image is separated in voids and solid part ; in the solid part, the fibre orientation is detected ; random walkers may circulate with specific rules in both parts of the image. Right: relative effective heat conductivity vs. temperature. The effect of radiation is visible only at very high temperatures.

The elementary mechanisms of heat transfer in CMCs may be not only conductive, but also may include radiation at high temperatures. In this case, the effective heat conductivity of the material is enhanced by radiation through the material pore network. To address this, we are currently developing a solver based again on random walkers, allowing for a coupled conductive (*i.e.* diffusive) / radiative transfer, the principle of which is illustrated in Figure 8. Simulated conduction in the solid accounts for the local anisotropy of the tows, and follows primarily the orientation

of the fibres, which has been detected by classical image analysis tools. Radiation is represented by ray tracing in the void parts of the images, the surface of which has been delineated under the form of a Simplified Marching Cubes [19] mesh. As a result, effective conductivities with and without radiation may be evaluated from the same image – in the case presented here, the effect of radiation on heat transfer is modest [20].

2.4 Self-healing simulations

The last part of the material cycle refers to its degradation and to the self-healing phenomenon. Here, the network of matrix cracks brings the oxygen in contact with all the inner material constituents; they are transformed gradually into oxides, some of them being gaseous (*e.g.* carbon), liquid (*e.g.* boron) or solid (*e.g.* silica at moderate temperatures). The calculation of the chemical reaction rate everywhere in the material is a key point for lifetime prediction. Past reports have described models which give the time evolution of the oxygen concentration in, say, some key part of the composite (*i.e.* the weakest, most exposed fibre); they deduce from this quantity a global lifetime because the tensile strength of this fibre can be related to oxygen exposure through a slow crack growth rate law [21]. These models were developed in 0 [22] or 1 [23] space dimensions. We propose now an image-based multi-dimensional approach, in which the resolution domain is a 2D FE mesh directly obtained from the fibre-scale mesh generation tools presented above. Oxygen diffusion, carbon consumption around the fibres and conversion of boron carbide into boron oxide are simulated [24]. The underpinning model consists of mass balances over oxygen (gaseous or dissolved), liquid phase height, boron-containing phase consumption height, and pyrocarbon consumed height. All the heights are considered perpendicular to the plane of the image, the latter assumed to be the crack plane (thin layer approximation). The results are distributions in space of the different heights, as well as the local oxygen concentration field. In particular, the point-wise oxygen concentration around each fibre is accessible. Figure 9 shows how the simulation works in a mesh obtained directly from a 2D transverse section of a tow, supposing that the image plane contains a crack bridged by the fibres. In the first moments of the cracks life, oxygen is consumed by the pyrocarbon interface present around all fibres, and oxygen depletion occurs; then, more slowly, the boron-containing phases begins to form glass, which eventually seals the crack. In the case of Figure 9, we can clearly see that the height of glass is directly related to the local oxygen concentration. Regions closer to the tow surface (hence to the oxygen source) show a faster and more effective oxidation, and consequently a greater height of glass. Such a numerical tool is able to help quantifying the contrasts in oxygen exposure in a single tow, and consequently to build less conservative estimations of the material lifetime.

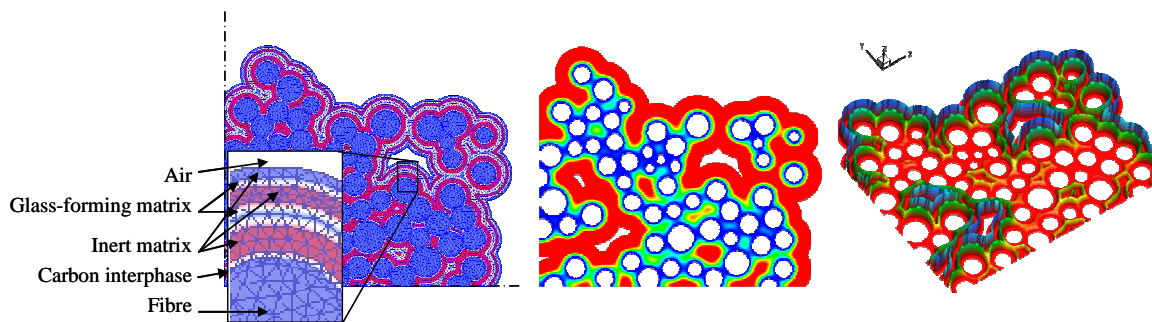


Figure 9. 2D modeling of oxidation in a crack of a SH-CMC. Left : FE mesh of the domain, with attribution of the different phases. A fixed oxygen partial pressure is assigned at all ceramic/air boundaries, and the unit cell is repeated by symmetry. Middle : oxygen concentration distribution before crack sealing. Right : distribution of liquid oxide height (amplified).

3. Conclusion and perspectives

We have introduced an integrated software suite aiming at a numerical multiscale simulation of the whole lifecycle of self-healing CMCs, featuring: (i) reinforcement weaving design, (ii) matrix infiltration, (iii) mechanical behaviour featuring damage, (iv) thermal behaviour, and (v) self-healing under oxidative gases. All simulations are developed in strong relationship with image analysis and synthesis, in order to provide a sound basis for experimental validation with respect to actual material samples. Numerical methods have been developed either on unstructured meshes or in voxel grid meshes (*i.e.* plain 3D images), or both. All simulations except matrix deposition by chemical vapour infiltration (CVI) have been developed in Finite Elements formulations; CVI and heat transfer have been coded in random walk algorithms.

This software suite can be used for prediction of the material behaviour as a function of its structural parameters and of the behaviour of each individual phase, thus providing a “virtual material toolbox” environment.

Of course, numerous improvements, tests, and validations have to be still performed, which are the object of ongoing and future work.

References

- [1] Christin, F., 2005. A global approach to fiber nD architectures and self-sealing matrices: from research to production, *Int. J. Appl. Ceram. Technol.* 2: 97 – 104.
- [2] Cavalier, J.C., I. Berdoyes, and E. Bouillon, 2006. Composites in aerospace industry. *Adv. Sci. Technol.* 50: 153–162.
- [3] Goujard, S., J.L. Charvet, J.L. Leluan, F. Abbé, and G. Lamazouade, 1995. Matériau composite protégé contre l'oxydation par une matrice autocicatrisante et son procédé de fabrication. French Patent N° 95 03606.
- [4] Kim, J.; Liaw, P. K.; Hsu, D. K., and McGuire, D. J., 1997. Nondestructive evaluation of Nicalon/SiC composites by ultrasonics and X-ray computed tomography, *Ceram. Eng. Sci. Proc.* 18(4): 287-296
- [5] Couégnat G., E. Martin and J. Lamon, 2009. Multiscale modelling of the mechanical behaviour of woven composite materials. In *17th International Conference on Composite Materials*, Edinburgh, UK, ID11.5 (10 p.)
- [6] Badel, P., E. Vidal-Salle, E. Maire, and P. Boisse; 2008. Simulation and tomography analysis of textile composite reinforcement deformation at the mesoscopic scale, *Compos. Sci. Technol.* 68(12):2433–2440.
- [7] Mulat, C., M. Donias, P. Baylou, G. L. Vignoles, and C. Germain, 2008a. Optimal orientation estimators for detection of cylindrical objects, *Signal Image and Video Processing* 2(1): 51-58.
- [8] Mulat, C., M. Donias, P. Baylou, G. L. Vignoles, C. Germain, 2008b. Axis detection of cylindrical objects in three-dimensional images, *J. of Electronic Imaging* 17(3): 0311081-0311089.
- [9] Couégnat, G., E. Martin, and J. Lamon, 2010. 3D multiscale modeling of the mechanical behavior of woven composite materials, *Ceram. Eng. Sci. Procs.* 31(2):185-194.
- [10] Vignoles, G. L., C. Mulat, C. Germain, O. Coindreau, and J. Lachaud, 2011. Benefits of X-ray CMT for the modelling of C/C composites, *Adv. Eng. Mater.* 13:178–185.
- [11] Vignoles, G. L., W. Ros, C. Mulat, O. Coindreau, and C. Germain, 2011. Pearson random walk algorithms for fiber-scale modeling of Chemical Vapor Infiltration, *Comput. Mater. Sci.* 50(3):1157-1168
- [12] Vignoles, G. L., C. Germain, O. Coindreau, C. Mulat, and W. Ros, 2009. Fibre-scale modelling of C/C processing by Chemical Vapour Infiltration using X-ray CMT images and random walkers, *ECS Transactions* 25(8): 1275-1284.
- [13] Vignoles, G. L., C. Germain, C. Mulat, O. Coindreau, and W. Ros, 2010. Modeling of infiltration of fiber preforms based on X-ray tomographic imaging, *Adv. Sci. Technol.* 71: 108-117.
- [14] Vignoles, G. L., W. Ros, I. Szelengowicz, and C. Germain, 2011. A Brownian motion algorithm for tow scale modeling of chemical vapor infiltration, *Comput. Mater. Sci.* 50(6) : 1871-1878.
- [15] Couégnat G., E. Martin and J. Lamon, Multiscale modelling of woven ceramic matrix composites based on a discrete micromechanical damage description, 2010. In *4th European Conference on Computational Mechanics*, Paris, France, CDROM ref. 1358 (2 p.)
- [16] Pineau, P., G. Couégnat, and J. Lamon, 2010. Virtual testing and simulation of multiple cracking in transverse tows of woven CMCs, *Ceram. Eng. Sci. Procs.* 31(2): 319-328.
- [17] Tomkova, B., M. Sejnoha, J. Novak, and J. Zeman, 2008. Evaluation of effective thermal conductivities of porous textile composites, *Int. J. for Multiscale Comput. Engng.*, 2:153–167.
- [18] El Yagoubi J. J. Lamon, J.-C. Batsale , 2010. Multiscale Modelling of the Influence of Damage on the Thermal Properties of Ceramic Matrix Composites, *Adv. Sci. Technol.* 73:65-71
- [19] Donias, M., G. L. Vignoles, C. Mulat, C. Germain, and J.-F. Delesse, 2011. Simplified Marching Cubes : an efficient discretization scheme for simulations of deposition/ablation in complex media. *Comput. Mater. Sci.* 50(3): 893-902.
- [20] Vignoles, G. L., J.-F. Bonnenfant, I. Szelengowicz, and L. Gélébart, 2010. Prédiction de la diffusivité thermique à haute température d'un composite SiCf/SiC : un outil numérique basé sur des marches aléatoires hybrides. In *Matériaux 2010 Conference CDROM*, 1526 (8 p.) (in French).
- [21] Gauthier, W., J. Lamon and R. Pailler, 2006. Fatigue statique de monofilaments et de fils SiC Hi-Nicalon à 500 et 800 °C, *Rev Compos Matér Avancés* 16(2): 221–241.
- [22] Cluzel, C., E. Baranger, P. Ladevèze, and A. Mouret, 2009. Mechanical behaviour and lifetime modelling of self-healing ceramic-matrix composites subjected to thermomechanical loading in air, *Composites Part A: Applied Science and Manufacturing* 40(8): 976-984.
- [23] Rebillat, F., 2005. Original 1D oxidation modeling of composites with complex architectures, In *HT-CMC 5 Conf. Procs.* 315-320.
- [24] Dréan, V., M. Ricchiuto, and G. L. Vignoles, 2010. Two-dimensional oxidation modelling of MAC composite materials, *INRIA Reports N°7417-7418* (in French).